# BMI-1 suppression increases the radiosensitivity of oesophageal carcinoma via the PI3K/Akt signaling pathway

XING-XIAO YANG[1], MING MA[2], MEI-XIANG SANG[3], XUE-YUAN ZHANG[1], ZHI-KUN LIU[1], HENG SONG[1] and SHU-CHAI ZHU[1]

Departments of [1]Radiation Oncology, [2]Clinical Laboratory and [3]Research Centre, The Fourth Hospital of Hebei Medical University, Shijiazhuang, Hebei 050011, P.R. China

**Abstract.** B-cell-specific Moloney murine leukaemia virus integration site-1 (BMI-1) contributes to the growth of tumour cells post-irradiation (IR). The aim of the present study was to characterize the effects of BMI-1 on cell viability, radiosensitivity and its mechanisms of action in oesophageal squamous cell cancer (ESCC). Western blotting and immunohistochemistry were employed to evaluate the protein expression of BMI-1 in ESCC cells and specimens, respectively. Additionally, the protein expression levels of BMI-1, H2AK119ub and γH2AX in ESCC cells were detected following different doses of IR and at different times after IR. The protein expression levels of MDC1 and 53BP1 were also measured. Flow cytometry and MTT assays were used to determine cell cycle progression, apoptosis and cell viability. The phosphatidylinositol 3-kinase inhibitor LY294002 and the agonist IGF-1 were employed to suppress or induce the phosphorylation of Akt to determine whether BMI-1 induces radioresistance in ESCC cells via activation of the PI3K/Akt pathway. The expression of BMI-1 was higher in ESCC tissues and cells compared with that in normal oesophageal tissues and cells. In addition, BMI-1 was positively related to tumour size and lymph node metastases and negatively to the overall survival of ESCC patients. IR induced the expression of BMI-1, H2AK119ub and γH2AX in a dose- and time-dependent manner. BMI-1 knockdown lowered the expression of γH2AX, MDC1 and 53BP1, suppressed cell viability and increased radiosensitivity. G2/M phase arrest was eliminated; this was followed by an increased proportion of cells entering the G0/G1 phase after IR and BMI-1 knockdown via the upregulation of P16 and downregulation of cyclin D2 and cyclin-dependent kinase-4. Moreover, BMI-1 knockdown increased cell apoptosis, downregulated MCL-1 and p-Akt and upregulated Bax. Additionally, the inhibitory effect of the downregulation of p-Akt by LY294002 on tumour cell viability was identical to that of BMI-1 knockdown, while the kinase agonist IGF-1 reversed the effects of BMI-1 knockdown on cell viability and radiosensitivity. Taken together, BMI-1 knockdown induces radiosensitivity in ESCC and significantly inhibits cell viability, which may contribute to an increased proportion of cells in the G0/G1 phase and cell apoptosis via suppression of the PI3K/Akt signalling pathway.

## Introduction

In China, there are ~0.4779 million new cases of oesophageal carcinoma (EC) each year (1). The most prevalent histologic type of EC is esophageal squamous cell carcinoma (ESCC) (2). Radiotherapy (RT) is an important strategy for treating EC, and it markedly improves survival rates. Although there have been considerable advances in EC therapy, poor prognosis is inevitable due to the rapidly proliferating tumour cells (3). Therefore, identification of the key molecules involved in ESCC may provide new therapeutic targets and further improve survival rates. It has been shown that multiple genetic alterations are closely associated with cell growth, metastasis and DNA damage repair in ESCC (4-5).

Epigenetic regulator polycomb group (PcG) genes are related to cell proliferation, invasion and migration. B-cell-specific Moloney murine leukaemia virus integration site-1 (BMI-1), the core component of PcG, is dysregulated in various types of cancers (6,7). BMI-1 is an important indicator for predicting cancer invasion (8), since it promotes cell viability, causes apoptosis resistance and enhances transfer capabilities according to gene chip analysis (9). Unfortunately, overexpression of BMI-1 is related to treatment failure in many malignancies, such as breast and prostatic cancer, and hepatocellular carcinoma (10-12). BMI-1 is known as a PcG protein and is required for H2AX ubiquitination-associated transcriptional silencing (13). Ubiquitylation of H2AX is likely activated by ATM kinase and causes H2AX phosphorylation at serine 139, followed by the recruitment of downstream genes, such as MDC1 and 53BP1, to the impaired sites and induction of the DNA damage response (DDR). MDC1 and 53BP1 are closely correlated with cell cycle arrest caused by

*Correspondence to:* Professor Shu-Chai Zhu, Department of Radiation Oncology, The Fourth Hospital of Hebei Medical University, 12 Jiankang Road, Shijiazhuang, Hebei 050011, P.R. China
E-mail: sczhu1965@163.com

the DDR. Inhibition of these molecules can delay the DDR and promote cell death (14,15). However, how BMI-1 is involved in radiosensitivity, particularly in the regulatory mechanisms of the DDR, is still unknown.

To identify the novel role of BMI-1 in the DDR of ESCC, a proteomic and molecular biology analysis was conducted to determine the function of this gene. To date, there have been few studies regarding the mechanism through which BMI-1 promotes cell viability in EC after RT, particularly studies including clinical and *in vitro* and *in vivo* data. There are also few studies regarding the regulatory effects of BMI-1 on the radiosensitivity of EC via the PI3K/Akt signalling pathway. Given the vital function of BMI-1 in DNA damage-induced DDR via the PI3K/Akt pathway, we hypothesized that BMI-1 knockdown may result in DDR defects and further increase radiosensitization by inactivating the PI3K/Akt pathway. In this article, different cell lines were used to verify this hypothesis *in vitro* and *in vivo*, as well as to further explore the regulatory mechanisms of BMI-1.

## Materials and methods

*Tissue specimens and immunohistochemical analysis.* Sixty ESCC and matched adjacent non-tumour tissues were collected at the Department of Thoracic Surgery, Hebei Hospital of the Fourth Affiliated Medical University (Hebei, China), from January 2010 to December 2010. Patient consent was obtained for the collection of specimens, and all study protocols were approved by the Ethics Committee for Clinical Research of the Fourth affiliated Medical University. Immunohistochemistry protocols were performed as previously described (16). Briefly, slides were incubated with an anti-BMI-1 monoclonal antibody (ab126783, 1:100; Abcam, Cambridge, MA, USA), and then with a horseradish peroxidase-conjugated anti-mouse secondary antibody (Dako, Glostrup, Denmark). Phosphate-buffered saline (PBS) was used instead of the anti-BMI-1 antibody for the negative control sections. Immunostaining results were independently evaluated by two pathologists. At least 4-5 random high-power fields (magnification, x200) from each section were observed. Positive samples were cases with >10% of cells staining for BMI-1 (17).

*Cell lines and cell culture.* The human normal oesophageal cell line HEEC and various human ESCC cell lines, including ECA109, KYSE30, EC9706 and TE13, were used for screening. These cells were obtained from the Research Center of the Fourth Hospital of Hebei Medical University (Shijiazhuang, China). To note, authentification of the TE13 cell line was verified by our laboratory. They were cultivated at 37°C and 5% $CO_2$ in RPMI-1640 medium (Gibco, Gaithersburg, MD, USA) supplemented with 10% foetal bovine serum (FBS) (Invitrogen, Carlsbad, CA, USA), penicillin (100 U/ml), and streptomycin (0.1 mg/ml).

*X-ray irradiation.* Post-irradiation (IR) was conducted using a 6-MV Siemens linear accelerator (Siemens, Concord, CA, USA) at a dose rate of 5 Gy/min. After that, cells were cultivated in an incubator before harvesting.

*shRNA transfection.* For the shRNA analyses, the sequences of shRNA against BMI-1 were: BMI-1 shRNA1, 5'-UCCUCA

UCCACAGUUUCCUCACAUU-3' (sense); BMI-1 shRNA2, 5'-GGGUCAUCAGCAACUUCUUCUGGUU-3' (sense); and BMI-1 shRNA3, 5'-GCUUAUCCAUUGAAUUCUUUGAC CA-3' (sense); and the negative control scrambled shRNA (NC-shRNA) sequence was: 5'-UUCUCCGAACGUGUCACG UTT-3' (sense); these sequences were designed and purchased from Invitrogen. Lipofectamine RNAiMAX (Invitrogen) was used to transfect the cells. Briefly, cells ($5x10^5$/well) were cultured in 6-well plates until they reached 50% confluency, and were then transiently transfected with either BMI-1-shRNA or NC-shRNA (100 nM). Cells were collected at 24 h after transfection with shRNA, followed by the selection of stable clones with puromycin and irradiation.

*Western blotting.* The cultured tumour cells or tissues were lysed in 500 $\mu$l of lysis buffer. The lysates were separated by sodium dodecyl sulfate polyacrylamide gel electrophoresis (SDS-PAGE) and were transferred onto polyvinylidene difluoride (PVDF) membranes. The PVDF membranes were incubated overnight with specific dilutions of the primary antibodies at 4°C. The antibodies included rabbit anti-human mAbs against BMI-1 (ab126783, 1:10,000), $\gamma$H2AX (ab26350, 1:1,000), MDC1 (ab114143, 1:800), 53BP1 (ab36823, 1:10,000), P16 (ab108349, 1:2,000), cyclin D2 (ab81359, 1:500), CDK4 (ab137675; 1:2,000), MCL-1 (ab32087, 1:3,000), and Bax (ab32503, 1:5,000) (Abcam) and anti-H2AK119ub (AB10029, 1:1,000) (Millipore, Billerica, MA, USA), rabbit anti-Akt (4685S, 1:1,000), anti-pAkt polyclonal (4058S, 1:1,000) (Cell Signaling Technology, Inc., Beverly, MA, USA) and $\beta$-actin (AP0060, 1:10,000) (Bioworld, Dublin, OH, USA) antibodies. The PVDF membranes were incubated with horseradish peroxidase-conjugated goat anti-rabbit secondary antibodies, followed by visualization using the Odyssey infrared imaging system. The levels of these proteins were calculated as the ratio of the intensity of the specified protein to that of $\beta$-actin.

*Cell viability assay.* MTT assays were performed to examine the effect of BMI-1 shRNA on cell viability (Sigma-Aldrich Chemical Co., St. Louis, MO, USA). Briefly, the transfected cells were cultured into a 96-well plate, followed by irradiation for 24 h. After incubation for 24, 48 and 72 h at 37°C, 5 $\mu$l of MTT reagent (5 mg/ml in PBS) was added to the cells, followed by incubation for 4 h. After that, the cells were incubated with 150 $\mu$l of dimethyl sulfoxide (DMSO) for 15-20 min. Absorbance at 492 nm was measured. This experiment was repeated 3 times. Cells were preincubated for 24 h with LY294002 and IGF-1 from Cell Signaling Technology (Beverly, MA, USA).

*Colony formation assay.* A standard colony formation assay was performed to generate cell survival curves (18). Graded single doses of IR (0-8 Gy) were used to irradiate tumour cells, followed by cultivation in RPMI-1640 supplemented with 10% FBS for 2 weeks. Then, the cells were fixed and stained with crystal violet (0.6%). The survival fraction was calculated according to a previous study (19). A single-hit multitarget formula was performed to analyse the data using GraphPad Prism 5 software: $S = 1 - (1 - e^{-D/D_0})^N$, where $D_0$ is the dose on the straight-line portion of the survival curve required to decrease the survival to 37%. The Dq, the intercept

of the extrapolated high dose, was calculated. N, the extrapolation number, was the measure of the width of the shoulder of the survival curve. SF after irradiation at 2 Gy ($SF_2$) and the sensitization enhancement ratio (SER) were obtained from the above parameters.

*Flow cytometry (FCM).* To assess the effects of BMI-1 shRNA on cell cycle progression and apoptosis, FCM was performed. The transfected cells were treated with IR for 24 h, and then harvested to analyse the cell cycle distribution. Cells were fixed with 70% ethanol at 4°C overnight, followed by washing with PBS and resuspension in staining solution for 30 min at room temperature in the dark. To measure cell apoptosis under different treatment conditions, cells were harvested and incubated with Annexin V and 7-AAD stains (BD Pharmingen™).

*Animals and tumour xenograft assay.* Stably transfected tumour cells were inoculated into the left hind paw of 4- to 6-week-old BALB/c nude mice. A dosage of 15 Gy was used to irradiate the mice for 21 days after the injection. To protect the upper part of the mice from irradiation, mice were placed in custom-made holders called a collimator container when irradiated. Tumour dimensions and volumes ($mm^3$) were measured and calculated with callipers once every week. In the end, the nude mice were sacrificed by cervical dislocation in the fifth week after exposure to irradiation and the tumors were harvested. Proteins were extracted from the tumor tissues and detected by western blotting (for Akt, pAkt). The other tumor tissues were fixed in formalin to obtain sections for the TUNEL assay and immunohistochemistry [for BMI-1 (ab126783, 1:100), Ki67 (27309-1-AP, 1:2,000) (ProteinTech Group, Inc., Chicago, IL, USA)]. The experimental protocols were evaluated and approved by the Animal Care and Use Committee of the Fourth Hospital of Hebei Medical University.

*Terminal deoxynucleotidyl transferase (TdT)-mediated dUTP nick end labeling (TUNEL) assay for cell apoptosis.* The DeadEnd™ System was employed to assay cell apoptosis. For detection of apoptosis in tissue sections, paraffin-embedded tissue sections were deparaffinized and permeabilized with proteinase K, and then coverslips were immersed in 4% paraformaldehyde for 25 min, 0.2% Triton X-100 in PBS for 5 min, and 100 µl equilibration buffer at room temperature for 5 min, followed by addition of 100 µl TdT reaction mix (98 µl equilibration buffer, 1 µl biotinylated nucleotide mix and 1 µl rTdT Eenzyme) and incubation at 37°C for 60 min. The coverslips were then immersed in 2X SSC for 15 min, 0.3% hydrogen peroxide for 3 min, and 100 µl streptavidin-HRP for 30 min, after which 100 µl DAB was added until a light brown background developed. The nuclei of apoptosis cells were stained dark brown. Quantitative analysis was performed blindly by counting the number of TUNEL-positive cells in 10 microscopic fields, as previously described. Apoptosis rate (%) = (apoptosis cells/total cells) (%).

*Statistical analysis.* SPSS software package version 13.0 (SPSS, Inc., Chicago, IL, USA) was used to conduct statistical analyses. All data are presented as the mean ± standard

Table I. Correlation between the expression of BMI-1 and clinicopathological variables of the patients with ESCC.

| Variables | BMI-1 expression | | P-value |
|---|---|---|---|
| | Positive | Negative | |
| Age, years | | | 0.448 |
| >60 | 18 | 13 | |
| ≤60 | 14 | 15 | |
| Gender | | | 0.755 |
| Male | 17 | 16 | |
| Female | 15 | 12 | |
| Tumour size (cm) | | | 0.022 |
| ≤5 | 10 | 17 | |
| >5 | 22 | 11 | |
| Histological grade | | | 0.466 |
| Good or moderate | 13 | 14 | |
| Poor | 19 | 14 | |
| TNM stage | | | 0.021 |
| I-II | 12 | 16 | |
| III-IV | 20 | 12 | |
| Lymph node metastasis | | | 0.011 |
| Positive | 23 | 11 | |
| Negative | 9 | 17 | |

BMI-1, B-cell-specific Moloney murine leukaemia virus integration site-1; ESCC, oesophageal squamous cell cancer; TNM, tumor-node-metastasis.

deviation (SD) of at least 3 independent experiments and were analysed by ANOVA. P-values of <0.05 and 0.01 were considered to indicate a statistically significant result.

**Results**

*BMI-1 is highly expressed in ESCC cells and specimens.* To evaluate BMI-1 expression, immunohistochemistry assays were performed on 60 ESCC and matched adjacent normal oesophageal tissues. In agreement with a previous study (20), BMI-1 was mainly expressed in the cell nuclei, but occasionally in the neoplastic epithelial cytoplasm and plasmalemma (Fig. 1A); its expression was observed in 32 of the 60 cases of oesophageal cancer (53.33%) (Table I). No staining or only weak staining was noted in normal epithelial cells. In addition, the expression of BMI-1 was measured in 30 pairs of ESCC and matched adjacent non-tumour tissues by western blotting (Fig. 1B). The expression of BMI-1 in tumour tissues was obviously higher than that of the corresponding normal oesophageal tissues (Fig. 1C; P<0.05), indicating that high expression of BMI-1 may result in the development and progression of ESCC.

Furthermore, 4 ESCC cell lines (EC9706, ECA109, KYSE30 and TE13) and the immortal oesophageal epithelial cell line HEEC were selected for measuring the expression of BMI-1 (Fig. 1D). The expression of BMI-1 was high in ESCC
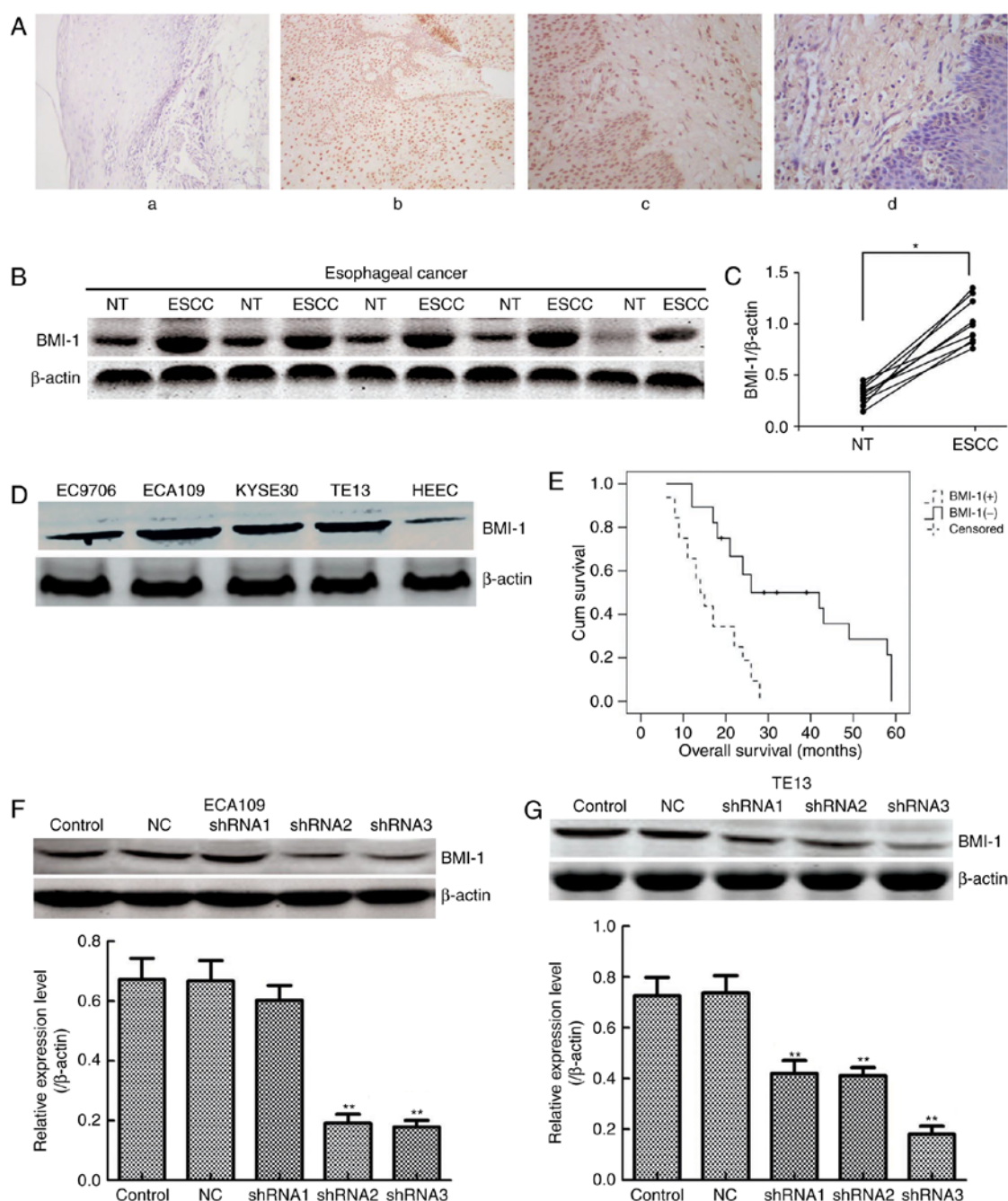
Figure 1. Expression of BMI-1 in ESCC tissues and cell lines. (A) Immunohistochemical staining of BMI-1 in normal oesophageal tissues (NT) and ESCC tissues. BMI-1 staining was mainly expressed in the nuclei and seldom in the cytoplasm and plasmalemma of cancerous cells. (a) Weak or absent BMI-1 in NT (magnification, x100); (b and c) strong BMI-1 staining in ESCC (b, magnification, x100; c, magnification, x200); (d) weak or absent BMI-1 in ESCC (magnification, x200). (B) The representative western blotting showing BMI-1 expression in 10 pairs of ESCC and non-tumour (NT) tissues. (C) The expression of BMI-1 was compared between ESCC and NT tissues in 10 patients; $^*$P<0.05. (D) The expression of BMI-1 in ESCC cells and HEEC by western blot analysis. The loading control was β-actin. (E) Kaplan-Meier overall survival curves for 60 patients with ESCC. The high expression of BMI-1 was related to a markedly shorter overall survival (P<0.001, log-rank test). (F and G) The expression of shBMI-1 was detected in ECA109 and TE13 cells by western blot assays, respectively; $^{**}$P<0.01.

cells, particularly ECA109 and TE13 cells. Collectively, the results of the western blot assays were in accordance with those of the IHC analyses, which supported that BMI-1 contributes to oesophageal carcinogenesis as an oncogene in oesophageal cancer.

*BMI-1 overexpression is related to the progression and poor prognosis of ESCC.* To explore the clinical significance of BMI-1 during ESCC development, the correlation between the expression of BMI-1 and the clinicopathological features of patients with ESCC were analysed. As shown in Table I, nuclear accumulation of BMI-1 in ESCC was markedly related to tumour size, clinical stage and lymph node metastasis (P<0.05), displaying a correlation between BMI-1 expression and cell proliferation and metastasis. However, no obvious correlation was observed between BMI-1 and patient age, sex or histological grade (P>0.05). Moreover, Kaplan-Meier survival analysis results indicated that patients harbouring low BMI-1 expression
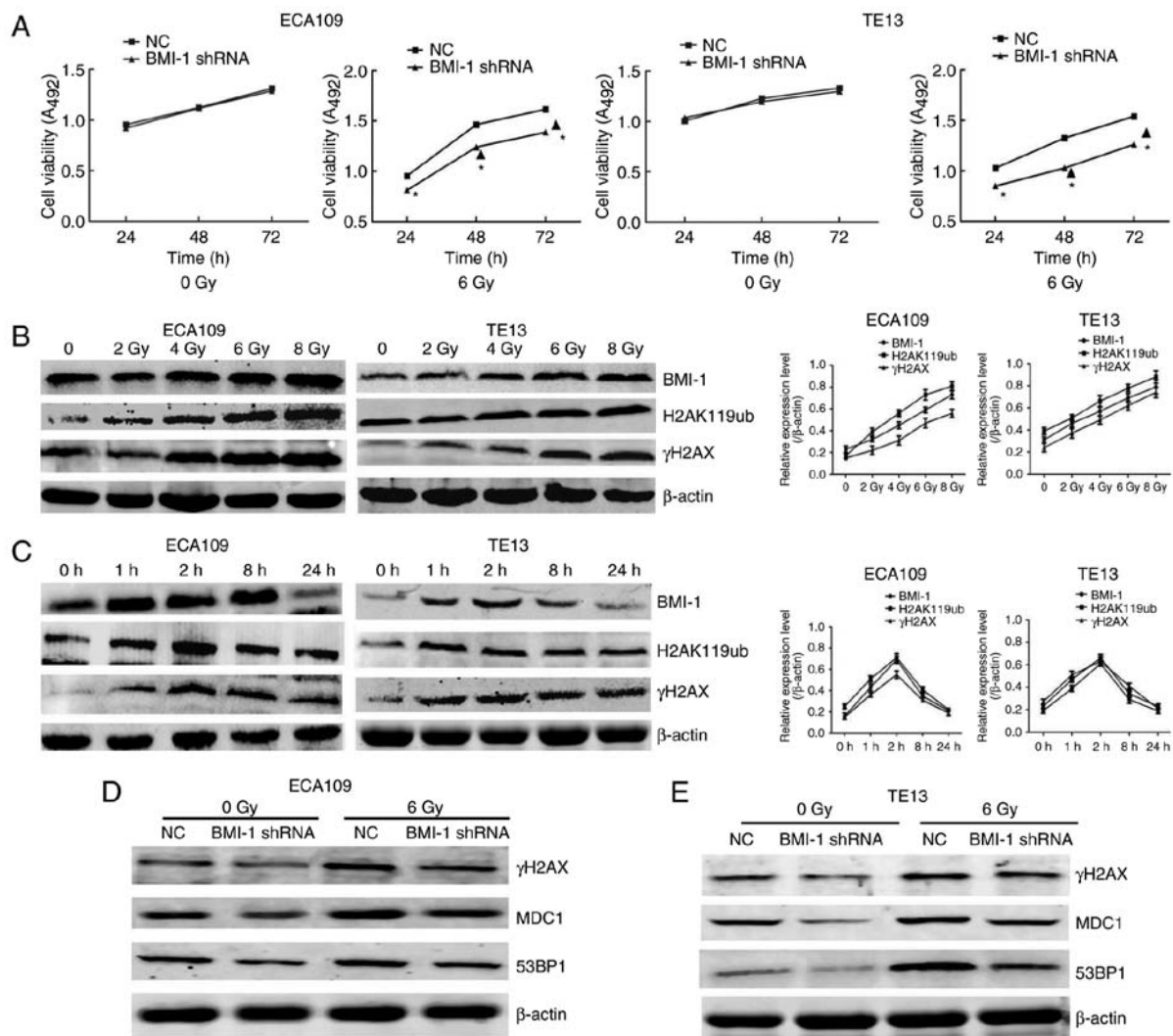
Figure 2. BMI-1 regulates cell viability and DNA damage repair genes, and enhances the radiosensitivity of oesophageal carcinoma cells *in vitro*. (A) The regulatory effect of shBMI-1 on cell viability of ECA109 and TE13 cells before and after IR. (B) The protein expression of BMI-1, H2AK119ub and γH2AX after treatment with 2, 4, 6 or 8 Gy at 1 h. Relative expression of above indexes to β-actin was detected at 1 h after irradiation with different doses in cells. (C) The protein expression of BMI-1, H2AK119ub and γH2AX after irradiated with 6 Gy at different times. Relative expression of above indexes to β-actin was detected at different times after IR in cells. (D) Western blot analysis was used to detect the expression of several DNA damage repair-related factors in ECA109 cells after treatment with BMI-1 shRNA or NC before and after IR. (E) Similar expression was detected in TE13 cells. The loading control was β-actin; *P<0.05 compared to the NC group; ▲P<0.05 compared to the corresponding unirradiated group.

had a markedly longer overall survival time than that of patients with high levels of BMI-1 (P<0.001, log-rank test; Fig. 1E). Collectively, the above results demonstrated that BMI-1 may be used to evaluate the prognosis of patients with ESCC.

*BMI-1 knockdown inhibits cell viability and promotes the radiosensitivity of ESCC cells after IR in vitro.* Either NC shRNA or shRNA targeting the BMI-1 gene was used to treat ECA109 and TE13 cells to reveal the important role of BMI-1. As shown in Fig. 1F and G, shRNA3 BMI-1 significantly inhibited the expression of BMI-1 in both cell types (P<0.01). Therefore, ECA109-BMI-1 shRNA3 and TE13-BMI-1 shRNA3 cells were further characterized.

To investigate the effect of BMI-1 knockdown on the growth of cells, MTT assays were employed to detect cell viability. As shown in Fig. 2A, cell viability was not markedly different in both groups of ECA109 and TE13 cells at the indicated time points before IR. In contrast, cell viability

was obviously increased after IR, particularly at 48 and 72 h (P<0.05), but BMI-1 knockdown markedly suppressed cell viability compared to the NC group (P<0.05). Additionally, radiosensitivity in both groups after IR was also detected. As shown in our previous study, the BMI-1 shRNA cells had greater radiosensitivity than that of the NC group (21). Collectively, our data suggested that IR combined with BMI-1 knockdown significantly inhibited cell viability and increased radiosensitivity *in vitro*.

*BMI-1 regulates DNA damage repair-related genes in a DNA damage-induced manner.* In the present study, IR promoted the expression of BMI-1, H2AK119ub and γH2AX at the protein level in a dose-dependent manner (Fig. 2B). Furthermore, the changes to these proteins were consistent in both cell types. The expression levels all reached their highest level at 1 and 2 h, and then gradually decreased (Fig. 2C). By 24 h, their levels were restored to unirradiated levels. These
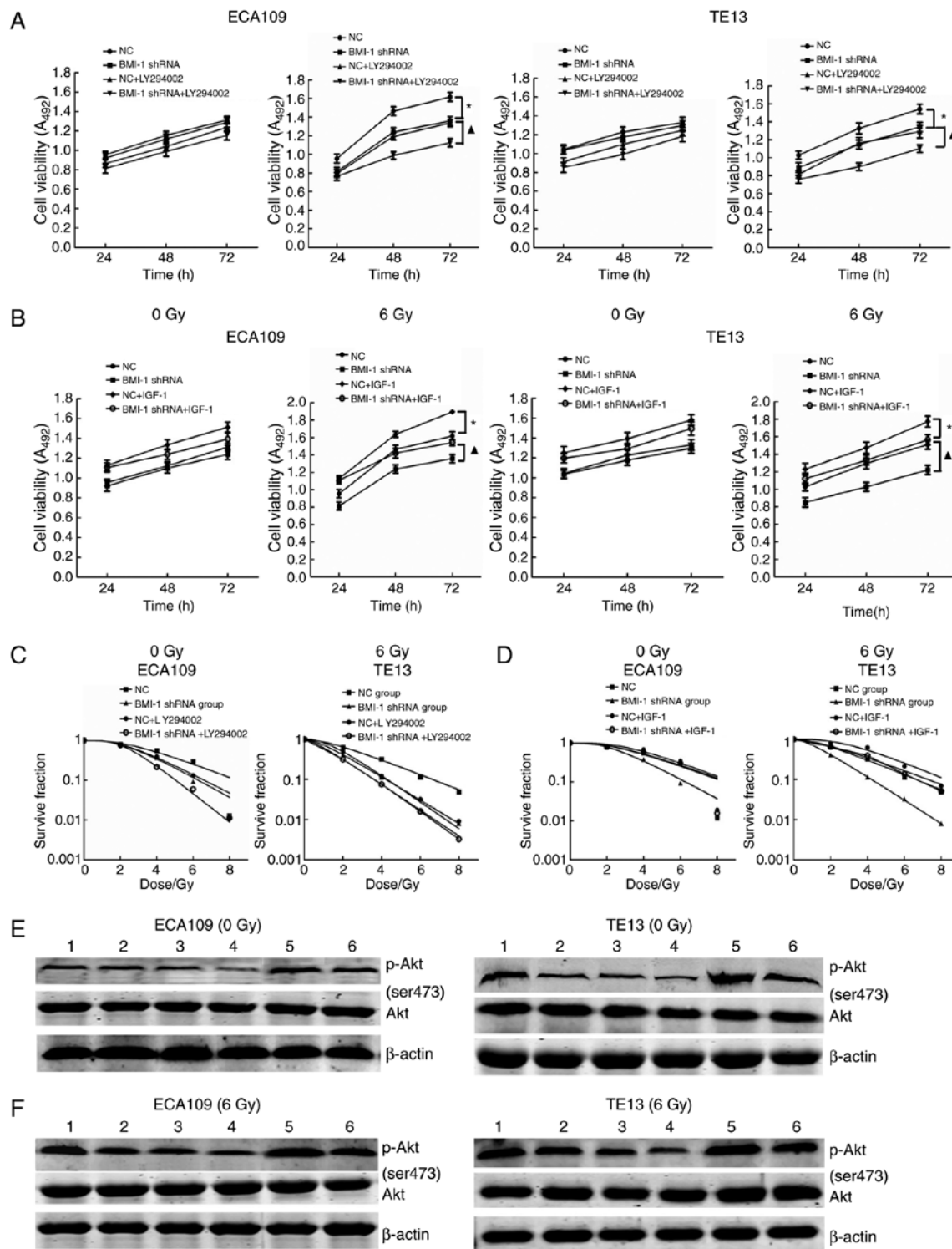
Figure 3. BMI-1 knockdown inhibits the growth of cells and improves the radiosensitivity of ECA109 and TE13 cells by inhibiting the PI3K/Akt pathway. (A) Effects of BMI-1 shRNA and LY-294002 on the cell viability of ECA109 and TE13 cells at different times by MTT assay. (B) Effects of BMI-1 shRNA and IGF-1 on the cell viability of ECA109 and TE13 cells at different times by MTT assay. (C) Effects of BMI-1 shRNA and LY-294002 on the radiosensitivity of ECA109 and TE13 cells at different doses by colony formation assay. (D) Effects of BMI-1 shRNA and IGF-1 on the radiosensitivity of ECA109 and TE13 cells at different doses by colony formation assay. (E) Western blot assay was employed to detect the effects of BMI-1 shRNA, LY-294002 and IGF-1 on the expression of Akt and p-Akt before IR in ECA109 and TE13 cells. (F) Effects of BMI-1 shRNA, LY-294002 and IGF-1 on the expression of Akt and p-Akt after IR in ECA109 and TE13 cells by western blot analysis. Lane 1, NC; lane 2, BMI-1 shRNA; lane 3, NC+LY-294002; lane 4, BMI-1 shRNA+LY-294002; lane 5, NC+IGF-1; lane 6, BMI-1 shRNA+IGF-1; *P<0.05 compared to NC group, ▲P<0.05 compared between BMI-1 shRNA and BMI-1 shRNA+LY-294002 or BMI-1 shRNA+IGF-1.

data led us to propose that there was a relationship between BMI-1 and H2AK119ub and γH2AX, which was in accordance with previous data that indicated that the interaction between

BMI-1 and H2AK119ub and γH2AX increased after IR as determined by co-immunoprecipitation (Co-IP) assay (21). In addition, we also evaluated the expression of γH2AX and its
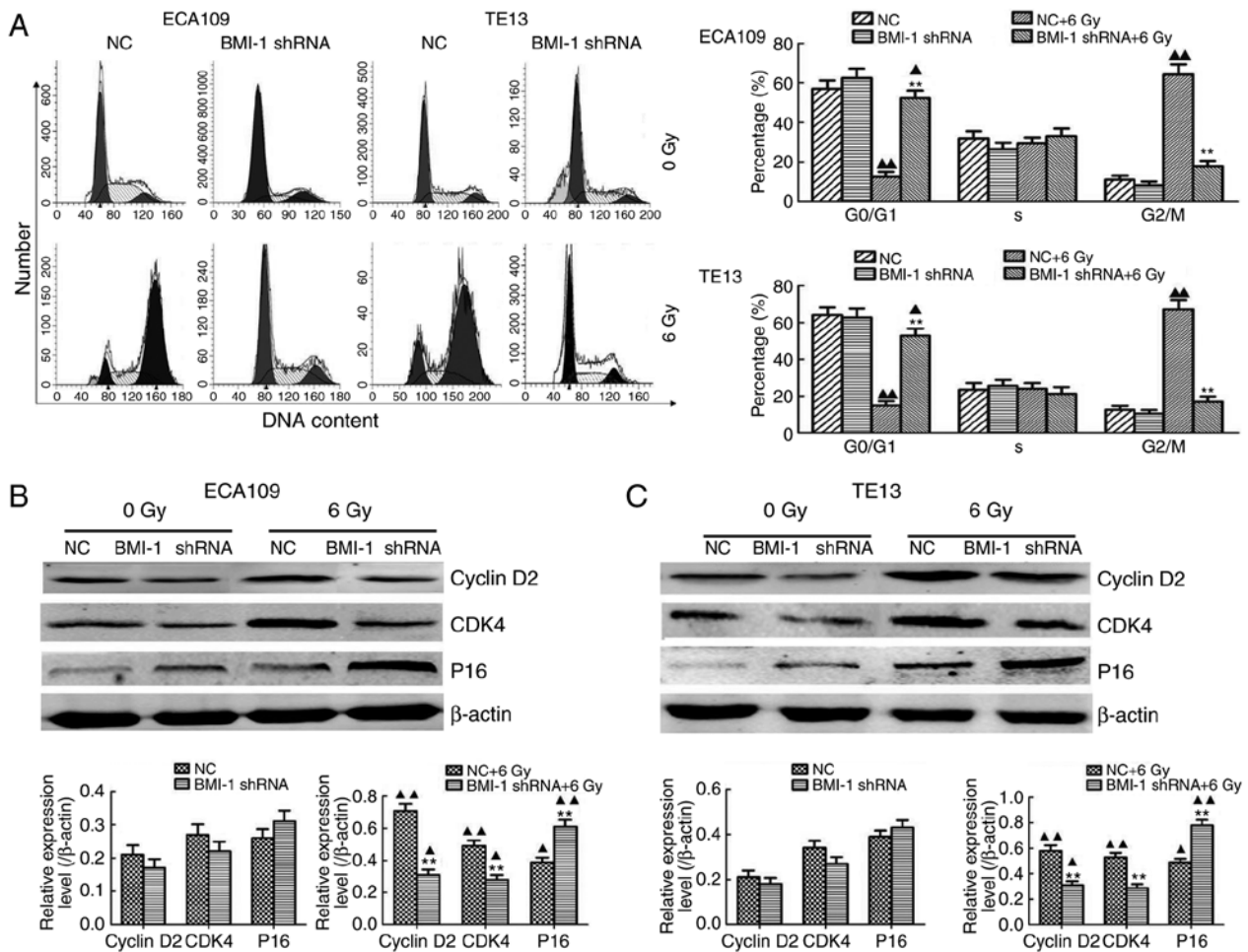
Figure 4. BMI-1 regulates the cell cycle of ESCC cells *in vitro*. (A) Cell cycling analysis of ECA109 and TE13 cells before and after IR by FCM. The distribution of the cell cycle is shown by quantitative analysis. (B) Western blot analysis was used to detect the expression of several cell cycle-related proteins in ECA109 cells after treatment with BMI-1 shRNA or NC before and after IR. Histogram of above indexes levels is shown as the mean ± standard error for each group in ECA109 cells. (C) Similar protein expression and histogram are shown in TE13 cells. The loading control was β-actin; **P<0.01 compared to the NC group; ▴P<0.05, ▴▴P<0.01 compared to the corresponding unirradiated group.

downstream genes, such as MDC1 and 53BP1, in the NC and BMI-1 shRNA groups after IR or not. Our results demonstrated that the levels of these indexes were not obviously altered before IR. Although IR induced the expression of γH2AX, MDC1 and 53BP1 in both groups, their protein levels were obviously lower in the BMI-1 shRNA group than those of the NC group in ECA109 (Fig. 2D) and TE13 cells (Fig. 2E) after IR. Collectively, our data suggested that BMI-1 regulates the expression of proteins associated with DNA damage repair, including γH2AX, MDC1 and 53BP1.

*BMI-1 silencing inhibits cell viability and improves radio-sensitivity in cells by inhibiting the PI3K/Akt pathway.* LY-294002 is a specific inhibitor of PI3K and can significantly inhibit the expression of p-Akt. After the addition of 20 mmol/l LY-294002, cell viability and the expression of p-Akt were decreased, and the radiosensitivity of the cells was increased, but was not significantly different from that of the BMI-1 shRNA and NC+LY-294002 groups with or without IR (all P>0.05); cell viability and the expression of p-Akt were significantly decreased, and the radiosensitivity of the cells was improved in the BMI-1 shRNA+LY-294002

group after IR compared with the BMI-1 shRNA group (P<0.05) (Fig. 3A, C, E and F).

IGF-1, as an agonist of PI3K, can activate PI3K and increase the expression of p-AKT. When 3 ng/ml IGF-1 was added to the cell culture medium, the effects of BMI-1 knockdown on cell viability and radiosensitivity were reversed. Cell viability and the expression of p-Akt were increased, and radiosensitivity was decreased but was not significantly different compared to that of the BMI-1 shRNA+IGF-1 and NC groups before and after IR (all P>0.05); cell viability and the expression of p-Akt were significantly increased, while the radiosensitivity of the cells was obviously decreased in the BMI-1 shRNA+IGF-1 group after IR compared with that of the BMI-1 shRNA group (P<0.05) (Fig. 3B, D, E and F).

*BMI-1 knockdown-mediated mechanisms of radiosensitization.* FCM was performed to explore the mechanisms involved in BMI-1 knockdown-mediated radiosensitization, and we demonstrated that IR obviously increased the proportion of cells in the G2/M phase of the cell cycle in both cell types *in vitro*; however, BMI-1 knockdown obviously decreased the proportion of cells in the G2/M phase (Fig. 4A) when considerable
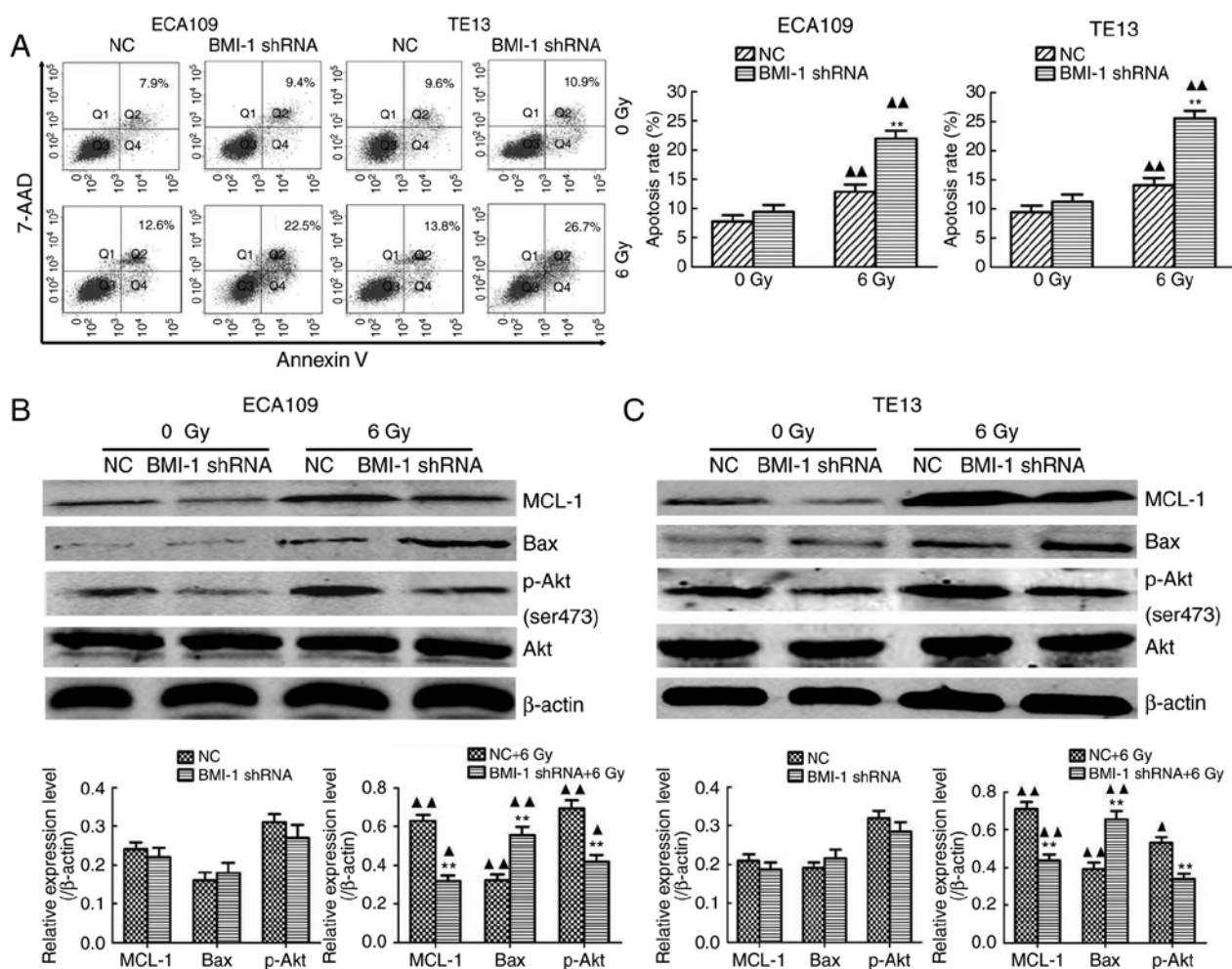
Figure 5. Apoptosis rates and the expression of protein associated with apoptosis in ECA109 and TE13 cells of the different groups *in vitro*. (A) The apoptosis rates are shown in both cells before and after IR. Histogram of apoptosis rates is shown as the mean ± standard error for each group. (B) The downregulation of MCL-1 and upregulation of Bax in ECA109 cells was significantly observed before and after IR. Histogram of above indexes levels is shown as the mean ± standard error for each group in ECA109 cells. (C) Similar protein expression and histogram are shown in TE13 cells; **P<0.01 compared to the NC group; ▲P<0.05, ▲▲P<0.01 compared to the corresponding unirradiated group.

time was allowed for the damage repair of tumour cells. This repair may decrease the killing effect of IR, thus inducing radio-resistance. However, the DDR was not significantly different in the both groups without IR. Collectively, our results showed that IR obviously induced cell cycle arrest at the G2/M phase, while BMI-1 knockdown decreased the proportion of cells in the G2/M phase to a certain degree, reducing the opportunity for tumour cells to repair, thereby improving radiosensitization. Moreover, the regulatory effect of BMI-1 on cell cycle-related proteins was detected by western blotting. Notably, their expression was detected before IR but was not obviously altered between the BMI-1 shRNA and NC groups. However, IR induced their expression in both groups. Although the expression of cyclin D2 and cyclin-dependent kinase 4 (CDK4) at the protein level was markedly inhibited, the expression of P16 was significantly increased in the BMI-1 shRNA group, compared to that of the NC group (P<0.05) (Fig. 4B and C).

Additionally, the apoptosis rate of both cell types in the BMI-1 shRNA group was slightly higher, compared to that of the NC group, but was not significantly different between the BMI-1 shRNA and NC groups before IR (all P>0.05). IR induced a dramatic increase in apoptosis, and BMI-1 knockdown

further promoted cell apoptosis after IR (P<0.01) (Fig. 5A). Moreover, IR induced the protein expression of MCL-1 and Bax. The expression of MCL-1 was downregulated, and the expression of Bax was upregulated after BMI-1 knockdown (P<0.01). However, their expression was not markedly altered before IR (Fig. 5B and C).

*BMI-1 knockdown inhibits the activation of the PI3K/Akt pathway.* As shown in Fig. 5B and C, BMI-1 silencing did not increase the total amount of Akt in either cell type before or after IR (P>0.05). The phosphorylation of Akt is a characteristic of PI3K activation. Compared with the NC group, the expression of p-AKT in ECA109 and TE13 cells in the BMI-1 shRNA group was slightly reduced, but was not significantly different before IR (P>0.05). IR induced the expression of phosphorylated Akt in each group (P<0.05) and BMI-1 knockdown markedly inhibited its expression (P<0.01).

*BMI-1 knockdown suppresses the tumour formation of oesophageal cancer cells in vivo.* TE13 cells in the BMI-1 knockdown and NC groups were inoculated into nude mice to determine the function of BMI-1 in tumour formation *in vivo*.
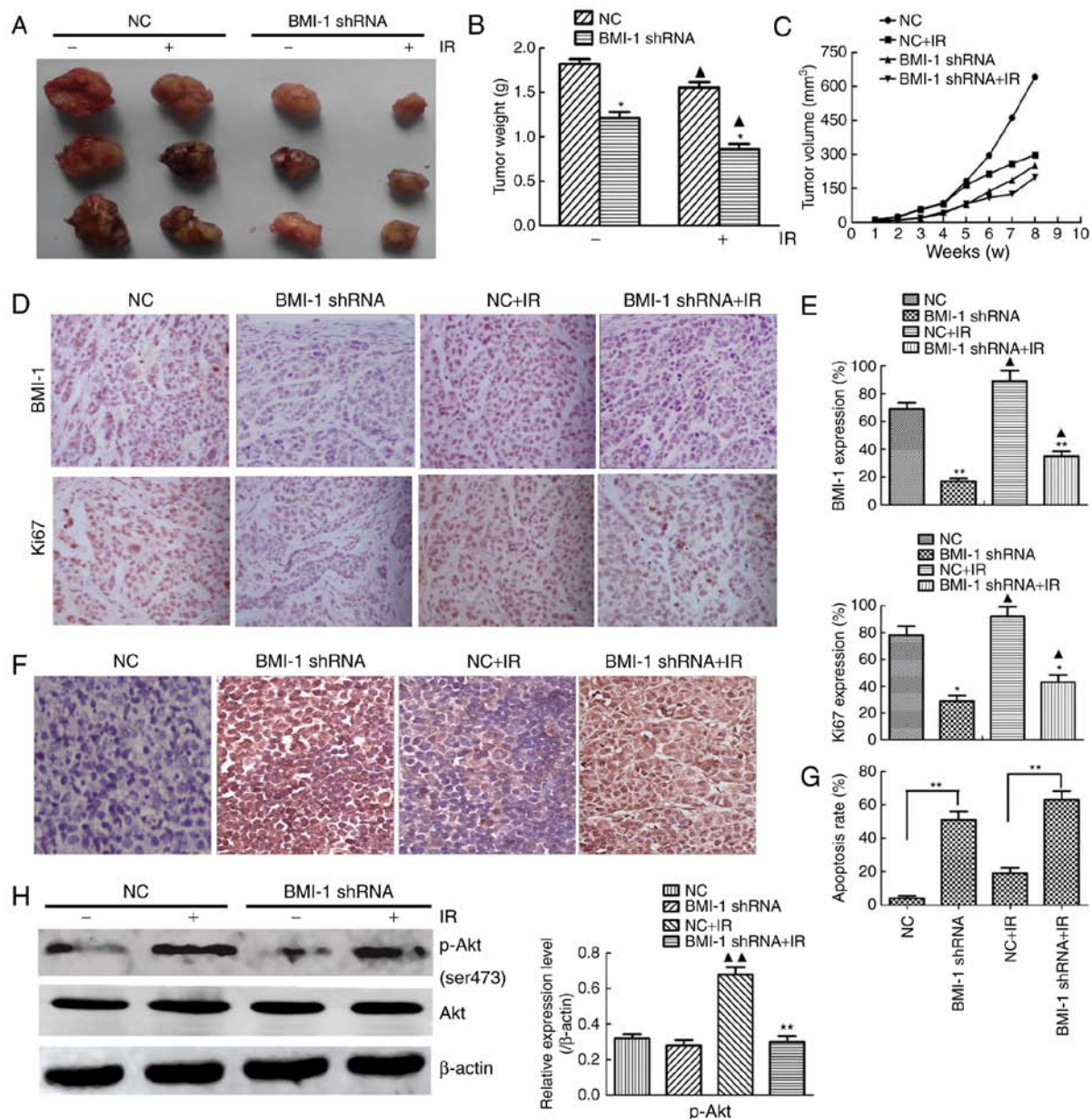
Figure 6. BMI-1 regulates the growth of ESCC cells *in vivo*. (A) At the end, we sacrificed the mice and dissected the tumours. Representative images from each treatment group are presented. (B) The net weights of tumour were measured before and after IR. The data are shown as the means ± standard error for each group. (C) Tumour growth curves of different groups in BALB/c nude mice. (D) Immunochemical staining for Ki67 and BMI-1 in the tumour xenografts (x200). (E) A semi-quantitative analysis of Ki67 and BMI-1 in the tumour xenografts. (F) Comparison of apoptosis levels in the 4 treatment groups by TUNEL staining. (G) Histogram of apoptosis rate is shown as the mean ± standard error for each group *in vivo*. The tumour in BMI-1 shRNA group had significantly increased cellular apoptotic levels after IR compared to NC group. (H) Western blot analysis of p-Akt is extracted from xenografts of nude mice treated as described; *P<0.05, **P<0.01 compared to NC group; ▲P<0.05, ▲▲P<0.01 compared to corresponding unirradiated group.

Although the NC and BMI-1 shRNA cells induced palpable tumours by 7 weeks after injection, the BMI-1 shRNA cells developed smaller tumours than those derived from the NC cells (Fig. 6A). BMI-1 knockdown did not affect cell viability *in vitro* before IR, but it markedly slowed tumour growth *in vivo*. Furthermore, IR caused smaller tumours, and the weights and volumes of tumours from the BMI-1 shRNA group were obviously lower compared to those of the other group after IR, indicating that BMI-1 knockdown may improve the radiosensitivity of oesophageal cancer *in vivo* (Fig. 6B and C).

The protein expression of BMI-1 and Ki67 in the tumour tissues was analysed by immunohistochemistry (Fig. 6D). IR induced the expression of Ki67 and BMI-1 in the tumour tissues, and the tumour tissues formed by the BMI-1 shRNA cells exhibited lower protein expression of Ki67 and BMI-1 than those formed by the NC cells before and after IR *in vivo*, which was different from the results *in vitro* (Fig. 6E), demonstrating that BMI-1 promoted tumour formation and the development of oesophageal cancer by accelerating the growth of cells *in vivo*.

To examine whether BMI-1 leads to cell apoptosis *in vivo*, we performed TUNEL assays in tumour tissues. These data demonstrated significantly higher apoptosis rates in the BMI-1 shRNA group before IR compared to those in the NC group (Fig. 6F and G), and this tendency was more obvious after IR (P<0.01). As shown in Fig. 6H, the expression of

p-Akt was downregulated in xenografts treated with shRNA and IR. The expression of p-Akt markedly increased in the NC group after IR compared with the corresponding unirradiated groups (P<0.01), but it was not markedly different in the BMI-1 shRNA group, regardless of IR (P>0.05).

## Discussion

It has been shown that BMI-1 is closely related to tumour radiosensitivity (22); it is involved in DNA damage repair, aberrant activation of multiple signalling pathways (23) and autophagy, all of which are involved in the complicated process of developing radioresistance. Given the ability of BMI-1 to regulate multiple oncogenic processes, including the response to RT, we considered investigation of the role of BMI-1 a promising avenue for furthering our understanding of radiation resistance. Therefore, any attempt to improve our understanding of the molecular mechanisms regarding radiosensitivity was the goal of the investigators.

In the present study, BMI-1 overexpression was observed in both ESCC-derived cell lines and ESCC tissues. Cell viability in both groups without IR was not significantly different, but cell viability in the BMI-1 shRNA group was slightly lower. However, the viability of ESCC cells in the BMI-1 shRNA group was significantly inhibited, and the radiosensitivity of the tumour cells was markedly improved after IR *in vitro*. This tendency was more obvious after BMI-1 silencing, indicating that IR combined with shRNA effectively gave rise to the suppression of cell viability and enhanced the radiosensitivity of the cells. Our data is in agreement with previous studies, which showed that BMI-1 knockdown inhibited the viability of cancer cells and further decreased their radioresistance and chemoresistance (7,24,25). A previous study demonstrated that BMI-1 was related closely to the ubiquitination and phosphorylation of H2AX (26). In agreement with the above results, our previous results from a co-IP assay revealed that the interaction between BMI-1 and H2AK119ub and γH2AX was significantly promoted in ESCC cells after IR, although there was no obvious interaction before IR, showing that IR induces the correlation between BMI-1 and the ubiquitylation and phosphorylation of H2AX (H2AK119ub and γH2AX) (21). To further explore their correlation, we measured their expression at different doses and times and found that IR induced similar dose- and time-dependent effects on the protein levels of BMI-1, H2AK119ub and γH2AX. Furthermore, BMI-1 knockdown resulted in decreased expression of important indexes of the DDR, such as γH2AX, MDC1 and 53BP1, confirming that BMI-1 contributed to the DDR through inducing the phosphorylation of H2AX (γH2AX) and its downstream targets, such as MDC1 and 53BP1, which play a vital regulatory role in the cell cycle.

PI3K/AKT, a signal transduction pathway, was most closely correlated with cell viability. Abnormal activation of the PI3K/AKT signalling pathway induced abnormal cell viability and differentiation and promoted the growth of tumour cells (27). Phosphorylation of Akt generated p-Akt, increased the expression of p-mTOR and p-70S6K through further activating the mTOR pathway, and ultimately increased cell viability (28). The present study found that BMI-1 knockdown can inhibit cell viability and reduce the expression of p-AKT. The changes were more obvious after IR. Then, we used LY-294002, a specific inhibitor of PI3K, to pre-treat ECA109 and TE13 cells and found that LY-294002 inhibited the expression of p-AKT and cell viability and improved radiosensitivity. Additionally, IGF-1, an agonist of PI3K, was also used to pre-treat ECA109 and TE13 cells. We found that IGF-1 significantly increased the expression of p-AKT and reversed the effects of BMI-1 knockdown on cell viability and radiosensitivity. This tendency was more obvious after IR. The results finally showed that BMI-1 knockdown inhibited the growth of cells and improved radiosensitivity by suppressing the PI3K/Akt pathway.

Additionally, IR increased the proportion of cells in the G2/M phase, but BMI-1 knockdown significantly eliminated this phenomenon after IR. However, without IR, the cell cycle distribution was not significantly different in either group. These results are in accordance with previous studies (29,30). To clarify whether BMI-1-mediated cell cycle arrest was involved in regulating cell cycle-related proteins, we investigated the expression levels of P16, cyclin D2 and CDK4 and found that BMI-1 knockdown resulted in a decrease in cyclin D2 and CDK4 expression and an increase in P16 expression. P16, a CDK inhibitor, negatively regulates cell cycle progression by binding various cyclin-CDK complexes and suppressing their viability (31). It has also been demonstrated that γH2AX, a marker of DDR, is closely associated with P16 and P53 (32,33). It has been reported that DNA damage induces the expression of P53 and P16, accompanied by increases in the proportion of cells in the G1 phase (34). In the presents study, BMI-1 knockdown downregulated the protein expression of cyclin D2 and CDK, upregulated the expression of P16, and altered the cell cycle distribution, suggesting that the effects of BMI-1 on tumour growth are correlated with increased cell viability via the regulation of some cyclins and P16, further regulating the cell cycle.

In addition to the cell cycle, the cellular response to DNA damage includes apoptosis. BMI-1 knockdown caused the suppression of cell viability and the induction of cell apoptosis, indicating that it may have a significant therapeutic effect on oesophageal carcinoma (35). Our data showed that IR markedly induced cell apoptosis and that BMI-1 knockdown facilitated this trend. However, cell apoptosis was not significantly different in either group without IR, but it was slightly higher in the BMI-1 shRNA group, thereby indicating the effect of BMI-1 knockdown on radiosensitization. Moreover, our results indicated that the effect of BMI-1 knockdown on promoting cell apoptosis after IR was accompanied by the downregulation of MCL-1 and the upregulation of Bax, which are related to cell apoptosis after DNA damage. The results of the present study are in agreement with previous studies (36,37). In addition to its effects on cell viability and radiosensitivity, the PI3K signalling pathway is a common mechanism involved in tumour cell metastasis and apoptosis (27,38,39). p-Akt is the core component of the PI3K signalling pathway, and its activation stimulates the growth of tumour cells (40). Therefore, full inactivation of p-Akt could be the key to enhancing radiosensitivity and promoting apoptosis in tumour cells. We found that high expression of BMI-1 after IR activated the PI3K/Akt pathway and promoted the expression of p-Akt, accompanied by the upregulation of MCL-1 and downregulation of Bax,

which were associated with radiosensitivity and apoptosis. In addition, BMI-1 knockdown suppressed the effect of PI3K/Akt on cell apoptosis, further suggesting that the PI3K/Akt signalling pathway is involved in BMI-1-mediated radioresistance.

Given the role of BMI-1 in oesophageal carcinoma *in vitro*, we explored whether the same effect appeared *in vivo*. It was shown that BMI-1 knockdown obviously suppressed the growth of tumours, including the weights and volumes, in nude mice after IR. The Ki67 index has been shown to be upregulated in many tumours, and its high expression is also significantly associated with decreased survival (41). The results demonstrated that IR induced the expression of BMI-1 and Ki67 in tumour tissues, but BMI-1 knockdown significantly decreased Ki67-positive cells in the tumours of nude mice. Additionally, BMI-1 knockdown also caused decreased expression of Ki67 before IR, which was different from the results *in vitro*, indicating that BMI-1 knockdown also inhibits cell viability *in vivo*. The reason for this may be that there were still certain non-specific immune functions in the nude mice, but no specific immune functions, in addition to the more complex microenvironment *in vivo*. Our TUNEL assay results revealed that IR induced apoptosis in nude mice, but the apoptosis rate was obviously increased after BMI-1 knockdown, indicating that inhibition of BMI-1 knockdown in oesophageal carcinoma is also mediated by the induction of apoptosis and thus increases radiosensitivity *in vivo*. We found that BMI-1 knockdown also downregulated the expression of p-Akt only *in vivo* and did not decrease the total amount of Akt, indicating that BMI-1 may contribute to radioresistance at least partly by activating the PI3K/Akt signalling pathway.

In summary, the present study demonstrated that BMI-1 was overexpressed in ESCC cells and was related to poor prognosis in ESCC patients. Moreover, BMI-1 knockdown decreased cyclin D2 and CDK4 expression, enhanced P16 expression, eliminated IR-induced G2/M cell cycle arrest, inhibited cell viability, improved radiosensitivity and induced apoptosis by inactivating the PI3K/Akt signalling pathway. To the best of our knowledge, we systematically demonstrated overall and systematically, that BMI-1 may be an important target gene for oesophageal carcinoma therapy.

## Acknowledgements

## References

1. Chen W, Zheng R, Baade PD, Zhang S, Zeng H, Bray F, Jemal A, Yu XQ and He J: Cancer statistics in China, 2015. CA Cancer J Clin 66: 115-132, 2016.
2. Ma M, Zhao LM, Yang XX, Shan YN, Cui WX, Chen L and Shan BE: p-Hydroxylcinnamaldehyde induces the differentiation of oesophageal carcinoma cells via the cAMP-RhoA-MAPK signalling pathway. Sci Rep 6: 31315, 2016.
3. Bertolini G, Roz L, Perego P, Tortoreto M, Fontanella E, Gatti L, Pratesi G, Fabbri A, Andriani F, Tinelli S, et al: Highly tumorigenic lung cancer CD133+ cells display stem-like features and are spared by cisplatin treatment. Proc Natl Acad Sci USA 106: 16281-16286, 2009.
4. Zhao JX and Xie XL: Regulation of gene expression in laryngeal carcinama by microRNAs. Int J Pathol Clin Med 32: 222-225, 2012.
5. Nacerddine K, Beaudry JB, Ginjala V, Westerman B, Mattiroli F, Song JY, van der Poel H, Ponz OB, Pritchard C, Cornelissen-Steijger P, et al: Akt-mediated phosphorylation of Bmi1 modulates its oncogenic potential, E3 ligase activity, and DNA damage repair activity in mouse prostate cancer. J Clin Invest 122: 1920-1932, 2012.
6. Ruan ZP, Xu R, Lv Y, Tian T, Wang WJ, Guo H and Nan KJ: Bmi1 knockdown inhibits hepatocarcinogenesis. Int J Oncol 42: 261-268, 2013.
7. Song W, Tao K, Li H, Jin C, Song Z, Li J, Shi H, Li X, Dang Z and Dou K: Bmi-1 is related to proliferation, survival and poor prognosis in pancreatic cancer. Cancer Sci 101: 1754-1760, 2010.
8. Bosch A, Panoutsopoulou K, Corominas JM, Gimeno R, Moreno-Bueno G, Martín-Caballero J, Morales S, Lobato T, Martínez-Romero C, Farias EF, et al: The Polycomb group protein RING1B is overexpressed in ductal breast carcinoma and is required to sustain FAK steady state levels in breast cancer epithelial cells. Oncotarget 5: 2065-2076, 2014.
9. Su WJ, Fang JS, Cheng F, Liu C, Zhou F and Zhang J: RNF2/Ring1b negatively regulates p53 expression in selective cancer cell types to promote tumor development. Proc Natl Acad Sci USA 110: 1720-1725, 2013.
10. Wang L, Liu JL, Yu L, Liu XX, Wu HM, Lei FY, Wu S and Wang X: Downregulated miR-495 [corrected] inhibits the G1-S phase transition by targeting Bmi-1 in breast cancer. Medicine 94: e718, 2015.
11. Jin M, Zhang T, Liu C, Badeaux MA, Liu B, Liu R, Jeter C, Chen X, Vlassov AV and Tang DG: miRNA-128 suppresses prostate cancer by inhibiting BMI-1 to inhibit tumor-initiating cells. Cancer Res 74: 4183-4195, 2014.
12. Yang F, Lv LZ, Cai QC and Jiang Y: Potential roles of EZH2, Bmi-1 and miR-203 in cell proliferation and invasion in hepatocellular carcinoma cell line Hep3B. World J Gastroenterol 21: 13268-13276, 2015.
13. Wang H, Wang L, Erdjument-Bromage H, Vidal M, Tempst P, Jones RS and Zhang Y: Role of histone H2A ubiquitination in Polycomb silencing. Nature 431: 873-878, 2004.
14. Ward IM, Minn K, van Deursen J and Chen J: p53 Binding protein 53BP1 is required for DNA damage responses and tumor suppression in mice. Mol Cell Biol 23: 2556-2563, 2003.
15. Moudry P, Lukas C, Macurek L, Neumann B, Heriche JK, Pepperkok R, Ellenberg J, Hodny Z, Lukas J and Bartek J: Nucleoporin NUP153 guards genome integrity by promoting nuclear import of 53BP1. Cell Death Differ 19: 798-807, 2012.
16. Li DQ, Qiu M, Nie XM, Gui R and Huang MZ: Oxidored-nitro domain-containing protein 1 expression is associated with the progression of hepatocellular carcinoma. Oncol Lett 11: 3003-3008, 2016.
17. Song LB, Zeng MS, Liao WT, Zhang L, Mo HY, Liu WL, Shao JY, Wu QL, Li MZ, Xia YF, et al: Bmi-1 is a novel molecular marker of nasopharyngeal carcinoma progression and immortalizes primary human nasopharyngeal epithelial cells. Cancer Res 66: 6225-6232, 2006.
18. Yang XX, Ma M, Sang MX, Wang XX, Song H, Liu ZK and Zhu SC: Radiosensitization of esophageal carcinoma cells by knockdown of RNF2 expression. Int J Oncol 48: 1985-1996, 2016.
19. Xie G, Zhan J, Tian Y, Liu Y, Chen Z, Ren C, Sun Q, Lian J, Chen L, Ruan J, et al: Mammosphere cells from high-passage MCF7 cell line show variable loss of tumorigenicity and radioresistance. Cancer Lett 316: 53-61, 2012.
20. Allegra E, Puzzo L, Zuccalà V, Trapasso S, Vasquez E, Garozzo A and Caltabiano R: Nuclear BMI-1 expression in laryngeal carcinoma correlates with lymph node pathological status. World J Surg Oncol 10: 206-211, 2012.
21. Yang XX, Sang MX, Zhu SC, Liu ZK and Ma M: Radiosensitization of esophageal carcinoma cells by the silencing of BMI-1. Oncol Rep 35: 3669-3678, 2016.
22. Dong Q, Sharma S, Liu H, Chen L, Gu B, Sun X and Wang G: HDAC inhibitors reverse acquired radio resistance of KYSE-150R esophageal carcinoma cells by modulating Bmi-1 expression. Toxicol Lett 224: 121-129, 2014.
23. Wang MC, Jiao M, Wu T, Jing L, Cui J, Guo H, Tian T, Ruan ZP, Wei YC, Jiang LL, et al: Polycomb complex protein BMI-1 promotes invasion and metastasis of pancreatic cancer stem cells by activating PI3K/AKT signaling, an ex vivo, in vitro, and in vivo study. Oncotarget 7: 9586-9599, 2016.

24. Liang W, Zhu D, Cui X, Su J, Liu H, Han J, Zhao F and Xie W: Knockdown BMI1 expression inhibits proliferation and invasion in human bladder cancer T24 cells. Mol Cell Biochem 382: 283-291, 2013.
25. Ma M, Zhao L, Sun G, Zhang C, Liu L, Du Y, Yang X and Shan B: Mda-7/IL-24 enhances sensitivity of B cell lymphoma to chemotherapy drugs. Oncol Rep 35: 3122-3130, 2016.
26. Ginjala V, Nacerddine K, Kulkarni A, Oza J, Hill SJ, Yao M, Citterio E, van Lohuizen M and Ganesan S: BMI1 is recruited to DNA breaks and contributes to DNA damage-induced H2A ubiquitination and repair. Mol Cell Biol 31: 1972-1982, 2011.
27. Zhang XJ, Yu HY, Cai YJ and Ke M: Lycium barbarum polysaccharides inhibit proliferation and migration of bladder cancer cell lines BIU87 by suppressing Pi3K/AKT pathway. Oncotarget 8: 5936-5942, 2017.
28. Fotouhi Ghiam A, Taeb S, Huang X, Huang V, Ray J, Scarcello S, Hoey C, Jahangiri S, Fokas E, Loblaw A, *et al*: Long non-coding RNA urothelial carcinoma associated 1 (UCA1) mediates radiation response in prostate cancer. Oncotarget 8: 4668-4689, 2017.
29. Liu WL, Guo XZ, Zhang LJ, Wang JY, Zhang G, Guan S, Chen YM, Kong QL, Xu LH, Li MZ, *et al*: Prognostic relevance of Bmi-1 expression and autoantibodies in esophageal squamous cell carcinoma. BMC Cancer 10: 467, 2010.
30. Min L, Dong-Xiang S, Xiao-Tong G, Ting G and Xiao-Dong C: Clinicopathological and prognostic significance of Bmi-1 expression in human cervical cancer. Acta Obstet Gynecol Scand 90: 737-745, 2011.
31. Boquoi A, Arora S, Chen T, Litwin S, Koh J and Enders GH: Reversible cell cycle inhibition and premature aging features imposed by conditional expression of p16Ink4a. Aging Cell 14: 139-147, 2015.
32. Blanco D, Vicent S, Fraga MF, Fernandez-Garcia I, Freire J, Lujambio A, Esteller M, Ortiz-de-Solorzano C, Pio R, Lecanda F, *et al*: Molecular analysis of a multistep lung cancer model induced by chronic inflammation reveals epigenetic regulation of p16 and activation of the DNA damage response pathway. Neoplasia 9: 840-852, 2007.
33. Wen W, Peng C, Kim MO, Ho Jeong C, Zhu F, Yao K, Zykova T, Ma W, Carper A, Langfald A, *et al*: Knockdown of RNF2 induces apoptosis by regulating MDM2 and p53 stability. Oncogene 33: 421-428, 2014.
34. Shapiro GI, Edwards CD, Ewen ME and Rollins BJ: p16$^{INK4A}$ participates in a $G_1$ arrest checkpoint in response to DNA damage. Mol Cell Biol 18: 378-387, 1998.
35. Yao XB, Wang XX, Liu H, Zhang SQ and Zhu HL: Silencing Bmi-1 expression by RNA interference suppresses the growth of laryngeal carcinoma cells. Int J Mol Med 31: 1262-1272, 2013.
36. Siddique HR, Parray A, Tarapore RS, Wang L, Mukhtar H, Karnes RJ, Deng Y, Konety BR and Saleem M: BMI1 polycomb group protein acts as a master switch for growth and death of tumor cells: Regulates TCF4-transcriptional factor-induced BCL2 signaling. PLoS One 8: e60664, 2013.
37. Zhu D, Wan X, Huang H, Chen X, Liang W, Zhao F, Lin T, Han J and Xie W: Knockdown of Bmi1 inhibits the stemness properties and tumorigenicity of human bladder cancer stem cell-like side population cells. Oncol Rep 31: 727-736, 2014.
38. Bussink J, van der Kogel AJ and Kaanders JH: Activation of the PI3-K/AKT pathway and implications for radioresistance mechanisms in head and neck cancer. Lancet Oncol 9: 288-296, 2008.
39. Deng R, Tang J, Ma JG, Chen SP, Xia LP, Zhou WJ, Li DD, Feng GK, Zeng YX and Zhu XF: PKB/Akt promotes DSB repair in cancer cells through upregulating Mre11 expression following ionizing radiation. Oncogene 30: 944-955, 2011.
40. Zhang Y, Zheng L, Ding Y, Li Q, Wang R, Liu T, Sun Q, Yang H, Peng S, Wang W, *et al*: *miR-20a* induces cell radioresistance by activating the *PTEN/PI3K/Akt* signaling pathway in hepatocellular carcinoma. Int J Radiat Oncol Biol Phys 92: 1132-1140, 2015.
41. Ji Y, Zheng MF, Ye SG, Chen J and Chen Y: PTEN and Ki67 expression is associated with clinicopathologic features of non-small cell lung cancer. J Biomed Res 28: 462-467, 2014.